Using optical tweezers to investigate the specific single-interaction between apoA-I molecule and ABCA1 on living cells

Jie Yu (余 杰)[1], Xunliang Tong (佟训靓)[2], Chengbin Li (李成彬)[1], Yining Huang (黄一宁)[2], and Anpei Ye (叶安培)[1*]

[1]*Key Laboratory for the Physics and Chemistry of Nanodevices, School of Electronics Engineering and Computer Science, Peking University, Beijing 100871, China*

[2]*Department of Neurology, Peking University First Hospital, Beijing 100034, China*

[*]*Corresponding author: yap@pku.edu.cn*

Received April 20, 2013; accepted May 31, 2013; posted online August 9, 2013

We carry out *in situ* single-molecule measurements of the specific interaction between apolipoprotein A-I (apoA-I) and ATP binding cassette transporter A1 (ABCA1) on THP-1 cells. Single-molecule force spectroscopy shows that similar to normal apoA-I, the dysfunctional apoA-I from diabetes patients interacts with ABCA1 via two different binding sites on the cells. The strength of dysfunctional apoA-I binding to a high-capacity binding site is 26.5±4.9 pN. The minor direct apoA-I/ABCA1 binding strength is 56.7±4.1 pN. These results facilitate a pathological understanding of the mechanisms that underlie the specific interaction of apoA-I and ABCA1 at the single-molecule level.

OCIS codes: 170.0170, 140.7010, 180.0180, 120.0120.

doi: 10.3788/COL201311.091701.

Optical tweezers are an effective tool for manipulating microbeads when measuring tiny displacements and minute forces of single molecules or individual living cells in the subpico-Newton range with high resolution[1−3]. Researchers have used this technique to study the mechanics of DNA and RNA, as well as the behaviors of molecular motors or entire cells[4−6]. In recent decades, scholars have extensively used optical tweezers to investigate specific receptor/ligand interactions by measuring the external force required to rupture a single molecular bond[7]. Important binding properties, such as binding strength, thermal dissociation rate, binding energy, and binding length, can be quantitatively obtained from the rupture–force spectrum[8]. Moreover, the use of optical tweezers has provided new insights into receptor/ligand systems. For example, these instruments have been used to characterize the specific interaction of BabA adhesin with its receptor Lewis b[9], the binding of monoclonal antibodies to tau peptides[10], and the binding behavior of several antigens and antibodies. Single-molecule force spectroscopy has become an important approach to revealing specific receptor/ligand binding properties; it advances the understanding of many biophysical issues[11].

Apolipoprotein A-I (ApoA-I) plays a crucial role in the human atheroprotective system. ApoA-I facilitates cellular lipid efflux through reverse cholesterol transport (RCT)[12]. ApoA-I functions by either directly forming a complex with the membrane lipid transporter, ATP binding cassette transporter A1 (ABCA1), or indirectly binding with a plasma membrane (PM) lipid domain created by ABCA1 activity[13]. The PM binding site contains a nearly 10-fold higher capacity to bind apoA-I over ABCA1 levels. Thus, the major binding site for apoA-I is also called the "high capacity binding site" (HCBS)[14]. Pathophysiologic studies reveal that either the dysfunctional apoA-I or ABCA1 may lead to metabolic abnormalities *in vivo* and increase the risk of cardiovascular complications in patients with diabetes mellitus[15]. Both proteins have become potential targets for therapies aimed at inhibiting the development of atherosclerotic vascular disease. The process of the specific binding of apoA-I to ABCA1 has been widely investigated by standard biochemical methods, such as the cross-linking method, immunoprecipitation, and autoradiography[16]. However, these approaches provide assessments on bulk samples. Underlying properties remain largely unknown, especially at the single-molecule level, because of the lack of appropriate high-resolution measurement techniques.

In this letter, optical tweezers are used to quantitatively investigate the interactions between the dysfunctional apoA-I of diabetes patients and ABCA1 on THP-1 cells in situ. Each of the three participants provides informed consent after the nature of the procedure was explained. The mechanism of the specific interaction is studied at the single-molecule level by single-molecule force spectroscopy.

Homemade optical tweezers were used for the measurements. A continuous-wave (CW) Nd:YAG laser (Compass 1064-2000N, Coherent, Germany) was directed into an inverted commercial microscope (Axiovert200, Zeiss, Germany) with a high numerical oil–immersion objective lens (Zeiss Aplan ×100, N.A. = 1.3) to form a stabilized three-dimensional optical trap. A microbead was trapped to serve as the sensitive probe. A custom-made quadrant photodiode detector (QPD) was placed conjugate to the back focal plane of the condenser lens. The QPD detects the motion of the probe by sensing changes in the intensity of the trapping laser and recording such intensity on a computer. The sample was precisely moved by a piezoelectric (PZT) stage (NIS-50, Nanonics, Israel; minimum step size, 0.64 nm) in all three dimensions. Manipulation and displacement measurements were simultaneously conducted, with an operating pro-

gram based on the LABVIEW software (National Instruments, Austin, TX). The entire procedure was visualized by a video charge coupled device camera (CCD; Cascade 512B, Roper Scientific, USA) in real time. To quantify the force F applied on the trapped probe, a two-step calibration for the system was initially performed. A detailed description is presented in a review of optical trapping[1]. All the assays were carried out at a trap stiffness of 0.25 pN/nm under the same conditions.

ApoA-I was isolated from human plasma high density lipoprotein (HDL), as previously described[17]. ApoA-I was covalently coupled to carboxyl-modified polystyrene microbeads (∼5 micron in diameter; Bangs laboratories, Inc. USA) for single-molecule force spectroscopy. During the process, the beads (10 μL; 3 600 μL^{-1}) were centrifuged (5 min, 5 000 rpm), harvested, and then incubated with apoA-I (20 μL; concentration, 0.145 mg/mL) for 2 h at room temperature. Redundant proteins in the solution were removed by washing with double distilled water (pH = 7.0). Bovine serum albumin (BSA) (500 μL; Sigma–Aldrich, Sweden) was added to block the unbounded carboxy1 sites on the beads. Afterward, the pretreated microbeads were stored at 4 °C until use. For nonspecific binding determination, the microbeads coated only with BSA were prepared as negative controls. The THP-1 cells were purchased from the Cell Resource Center of IBMS, CAMS/PUMC (Beijing, China), and cultured for 30 to 40 h with RPMI-1640 medium, supplemented with 12.5% phosphate-buffered saline, 2-mM L-glutamine, 100-μg/mL penicillin/streptomycin (M&C Gene Tech. Ltd., China), and 10% fetal calf serum at 37 °C in a humidified atmosphere (5% CO_2 in air). The mouse anti-ABCA1 monoclonal antibody, ab18180, was purchased from Abcam Company (Cambridge, UK). It was pre-incubated with THP-1 cells (30 min) to block the specific binding sites of apoA-I on the cell surface in the blocked group.

In the experiment, the THP-1 cells (20 μL) and beads(20 μL) were placed into the sample pool that was held on the PZT stage in the optical tweezer system. A naturally settled cell was moved for contact with the trapped probe (Fig. 1, inset). After transient contact, the cell was retracted with a constant speed of 20 μm/s until binding departure. The likelihood of effective adhesion was affected by contact area, contact time, and appropriate binding orientation[18]. To ensure binding formation, the cell was driven to slightly push on the probe before retraction[19]. The typical force curve detected by the QPD is displayed in Fig. 1, which shows that a binding rupture occurs and are extracted from the force curves. According to the Bell–Evans theory of bond kinetics, the external force applied to a bond increases the dissociation rate, which can be described by[20,21]

$$k(F) = k_0 \exp\left(\frac{Fx_\beta}{k_\mathrm{B}T}\right), \tag{1}$$

where k_0 is the intrinsic dissociation rate, x_β is the characteristic length between the ground state and the transition states, F is the applied external force, k_B is the Boltzmann constant, and T is the absolute temperature. The maximum distribution of the binding rupture force induces specific binding strength F_b (or alternatively, the most likely force), which is logarithmic ally related to pulling rate r[22]:

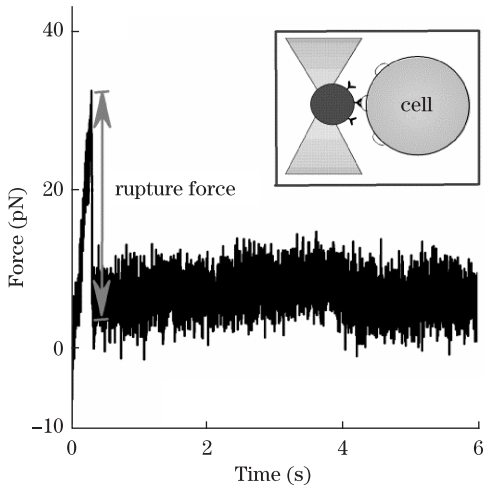

Fig. 1. Typical force curve detected by QPD, in which a binding rupture is observed. Inset is the schematic of a specific binding measurement. A naturally settled cell is moved for contact with the trapped bead. After the initial contact, the cell is driven to leave at a certain speed until the bond ruptures.

$$F_\mathrm{b} = \frac{k_\mathrm{B}T}{x_\beta} \ln\left(\frac{x_\beta \times r}{k_\mathrm{B}T \times k_0}\right). \tag{2}$$

The binding kinetic parameters, such as bond length and dissociation rate, can be predicted by this relationship[23].

The results are based on 895 single-molecule apoA-I/ABCA1 binding events (functional group), 395 binding circles of apoA-I to antibody-blocked THP-1 cells (blocked group), and 310 negative control tests conducted between the beads coated only with BSA and the THP-1 cells (negative control group). The values are presented as means±SD. The statistical differences were analyzed using the nonpaired t-test. A P value < 0.05 is considered statistically significant.

The specific molecular interaction between apoA-I and ABCA1 was revealed by the binding frequencies. The dysfunctional apoA-I binds to the THP-1 cells with a binding frequency of 32.9%±4.5% in the functional group (bar A, Fig. 2). According to Poisson statistics, when 30% of the approach/retraction cycles lead to receptor/ligand binding, 83% of these successful adhesions are probably contributed by single binding events[24]. This phenomenon indicates that the interaction between the dysfunctional apoA-I and THP-1-expressing ABCA1 is measured at the single-molecule level. The binding frequency in the blocked group drastically decreases to 14.4%±3.7% (bar B) because of antibody function. Nonspecific interactions arising from Van der Waals forces, hydrogen bonding, hydrophobic forces, and electrostatic attractions between the microbeads and cells contribute to a few weak bindings in the negative control group. These background interactions result in a binding frequency of 7.9%±2.8% (bar C), which is lower than that achieved in the functional group. On the basis of these results, the specificity of dysfunctional apoA-I binding to ABCA1 on THP-1 cells can be confirmed at the single

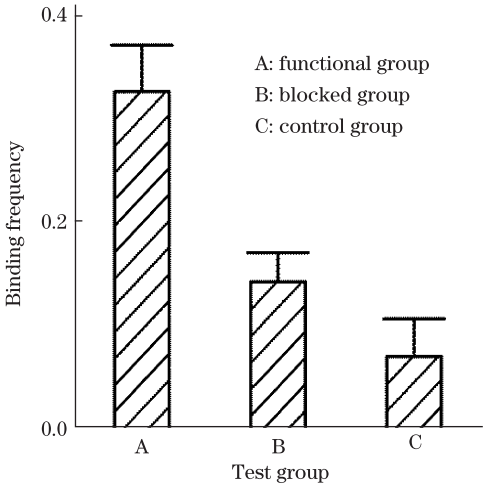

Fig. 2. The binding frequencies of the three groups reveal the specific interaction between apoA-I and ABCA1 on THP-1 cells. A shows the interaction between dysfunctional apoA-I and ABCA1 on THP-1, with a binding frequency of 32.9%±4.5%. This result indicates the specificity of dysfunctional apoA-I/ABCA1 interaction at the single-molecule level. B shows the frequency of apoA-I binding to anti-ABCA1 antibody-blocked THP-1 cells (14.4%±3.7%). The binding frequency of the negative control group is 7.9%±2.8% in C, which represents background nonspecific attractions.

interaction level, which is in accordance with the findings that Vedhachalam *et al*. determined by cross-linking and SDS-PAGE methods[13].

As indicated by Abcam's protocol, the antibody works on the C terminus (amino acids 1800–2260) of human ABCA1, which determines the stability of ABCA1. Michael *et al.*[25] showed that the C terminus of the ABCA1 does not physically associate with apoA-I. In addition, the function of the C terminus of the ABCA1 in the stability of ABCA1 by the HCBS was proposed by Iulia *et al.*[15]. Our results indicate that the frequency at which the dysfunctional apoA-I binds to the intact THP-1 cells is higher than that at which antibody blocked cells bind to the cells; combining the findings from the aforementioned studies and our results enables the verification of the specific binding of dysfunctional apoA-I to the HCBS. Although inhibited by the antibody, the blocked group exhibits a higher binding frequency than does the negative control group. That is, not all the apoA-I/ABCA1 interactions are restrained by the antibody, raising the issue of whether the direct apoA-I/ABCA1 association plays a role in the interactions. Therefore, we analyzed the rupture–force distributions to obtain deeper insight into the specific interaction between the (or the near?) dysfunctional apoA-I and ABCA1 on the THP-1 cells.

The rupture-force distribution of the functional group is shown in Fig. 3(a). The bin width w of the histogram was determined according to Scott's choice[26]: $w = 3.5\sigma/\sqrt[3]{N}$, where N is the sample size and σ is the standard deviation of the entire forces. Given that the interplay between specific and nonspecific interactions may distort the rupture–force distribution, and further affect the binding kinetics, this histogram cannot exactly describe the specific interaction between apoA-I and ABCA1. Thus, we eliminated the influence of the nonspecific interactions on the histogram of the functional group. We assumed that the specific and nonspecific interactions additively contribute to the binding rupture–force distribution[10], enabling their separation through the subtraction of the histograms. Through this process, the relatively weak nonspecific interactions and experimental errors can be removed. The larger bin size was chosen and applied to both sample sets. After normalization, every fraction of the histograms was weighted to their respective binding frequency (0.329, 0.079). Figure 3(b) shows the rupture–force distribution of the negative control group, which represents the nonspecific interaction between the microbeads and THP-1 cells.

The difference, which corresponds to the specific interaction of the dysfunctional apoA-I with ABCA1 on the THP-1 cells, is shown in Fig. 3(c). The maximum occurs 26 pN in the corrected histogram, and its probability slightly diminishes. Moreover, a small accumulation occurs at around 50 pN. Given that the few force curves with multiple binding ruptures were discarded before statistical analysis to ensure single binding event measurement, this accumulation may not represent multiple apoA-I/ABCA1 bond dissociations. Instead, this condition may result from other binding sites for apoA-I on the THP-1 surface, aside from the HCBS. To further confirm its existence, we processed the rupture–force distribution of the blocked group following the same procedure.

Figure 4(a) shows the resultant interaction between the dysfunctional apoA-I and antibody-blocked THP-1 cells. Major apoA-I/HCBS binding events are visibly restrained by the antibody, removing a weak affinity. A theoretical Gaussian distribution curve was applied to the histogram. A single peak with a relative frequency of 3.7%±3.2% was obtained at 56.7±4.1 pN, suggesting the existence of a remaining binding site for apoA-I.

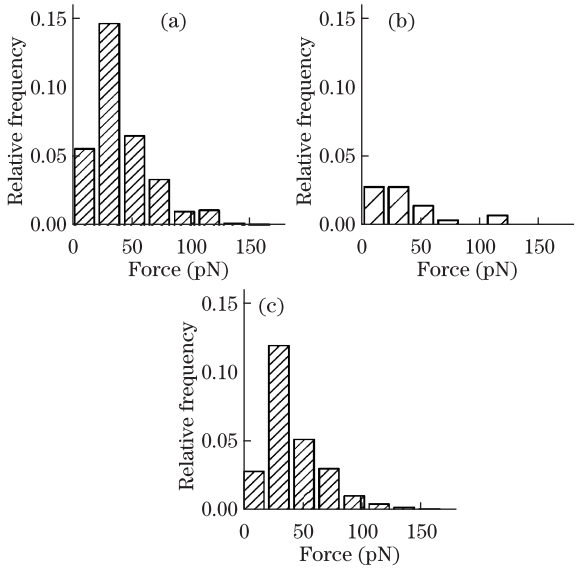

Fig. 3.(a) Normalized weighted rupture-force distribution in the functional group. (b) Rupture-force distribution in the negative control group. By subtracting the histograms, the nonspecific interactions in the functional group are minimized. (c) Corrected rupture-force distribution of specific apoA-I/ABCA1 interaction. A major peak is obtained in the histogram.

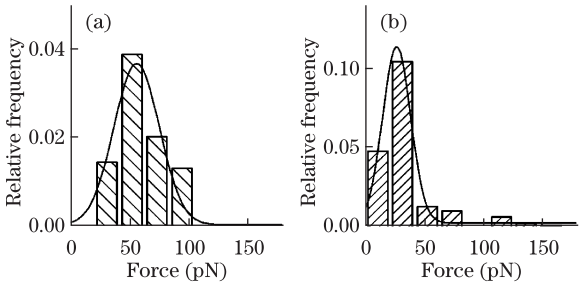

Fig. 4. (a) Rupture–force distribution in the blocked group. A single peak at 56.7±4.1 pN is obtained from the theoretical Gaussian curve, which reflects the minor direct binding of apoA-I to ABCA1. (b) Rupture–force distribution that corresponds to the interaction of apoA-1/HCBS. The binding strength is determined from the single peak (26.5±4.9 pN).

Afterward, the major apoA-I/HCBS interaction was extracted from the histogram of the functional group by subtracting the histogram of the blocked group. The specific apoA-I/HCBS binding is illustrated in Fig. 4(b). The theoretical Gaussian distribution curve was applied, and the strength of apoA-I binding to the HCBS was determined (26.5±4.9 pN). The relative frequency at the peak is 10.8%±4.3%. As previously stated, normal apoA-I interacts with ABCA1 through two binding sites, thereby facilitating cellular lipid efflux. These results show that similar to normal apoA-I, the dysfunctional apoA-I also interacts with ABCA1 on the cell surface through two binding sites. Only a tiny fraction of apoA-I is directly associated with ABCA1, and most apoA-I proteins target the HCBS. Furthermore, we can deduce that the minor direct binding of the dysfunctional apoA-I to ABCA1 shows strong attraction. Meanwhile, the prominent binding of apoA-I to the HCBS is relatively weak. Our data also show that the binding capacity of apoA-I/HCBS is nearly threefold higher than that of the direct apoA-I/ABCA1 association, whose value is lower than the ratio of normal apoA-I[13]. This result suggests that the binding of the dysfunctional apoA-I from patients to the HCBS may have been partially impaired, an issue that requires further investigation.

In conclusion, we study the specific interaction between dysfunctional apoA-I and ABCA1 on single living cells by using optical tweezers. Our analysis shows that the dysfunctional apoA-I of diabetes patients comes into contact with ABCA1 on THP-1 cells through two binding sites, as in that observed in normal apoA-I. The binding strengths are determined by single-molecule force spectroscopy analysis. The strength of apoA-I binding to the HCBS is weaker than that observed under the direct binding mode. The apoA-I/HCBS interaction, which is consistently higher than the direct apoA-I/ABCA1 association, may exhibit decline in patients, indicating that the binding ability of apoA-I to the HCBS may have been partially impaired. The detailed mechanisms that underlie apoA-I interactions with ABCA1 or the HCBS require more extensive study. Binding properties, such as thermal dissociation rate and binding length, can also be further explored. The results indicate that optical tweezers can serve as extraordinary tools for exploring the specific interactions between biological macromolecules at the single-molecule level.

This work was supported by the National Basic Research Program of China (No. 2011CB809100), the National Science and Technology Infrastructure Program of China (No. 2012BAF14B14), and the National Key Technologies R&D Program of China (No. 2012ZX09303005003).

References

1. K. C. Neuman and S. M. Block, Rev. Sci. Instrum. **75,** 2787 (2004).
2. A. Rohrbach, C. Tischer, D. Neumayer, E.-L. Florin, and E. H. K. Stelzer, Rev. Sci. Instrum. **75,** 2197 (2004).
3. T. Tao, J. Li, Q. Long, and X. Wu, Chin. Opt. Lett. **9,** 120010 (2011).
4. S. Jeney, E. H. K. Stelzer, H. Grubmüller, and E.-L. Florin, Chem. Phys. Chem. **5,** 1150 (2004).
5. H. Zhang and K. K. Liu, J. Roy. Soc. Interface. **5,** 671 (2008).
6. M. Zhong, G. Xue, J. Zhou, Z. Wang, and Y. Li, Chin. Opt. Lett. **10,** 101701 (2012).
7. D. Leckband, Annu. Rev. Biophys. Biomol. Struct. **29,** 1 (2000).
8. Y. Xiong, A. Ye, C. Wen, and Y. Zhang, Chin. Opt. Lett. **8,** 1015 (2010).
9. O. Björnham, J. Bugaytsova, T. Borén, and S. Schedin, Biophys. Chem. **143,** 102 (2009).
10. C. Wagner, D. Singer, O. Ueberschär, T. Stangner, C. Gutsche, R. Hoffmann, and F. Kremer, Soft Matter **7,** 4370 (2010).
11. D. Leckband, Annu. Rev. Chem. Biomol. Eng. **1,** 365 (2010).
12. J. F. Oram, Arterioscler. Thromb. Vasc. Biol. **23,** 720 (2003).
13. C. Vedhachalam, A. B. Ghering, W. S. Davidson, S. Lund-Katz, G. H. Rothblat, and M. C. Phillips, Arterioscler. Thromb. Vasc. Biol. **27,** 1603 (2007).
14. H. H. Hassan, M. Denis, D. Y. Lee, I. Iatan, D. Nyholt, I. Ruel, L. Krimbou, and J. Genest, J. Lipid Res. **48,** 2428 (2007).
15. I. Iatan, D. Bailey, I. Ruel, A. Hafiane, S. Campbell, L. Krimbou, and J. Genest, J. Lipid Res. **52,** 2043 (2011).
16. D. S. Ory and J. E. Schaffer, Diabetes **59,** 2358 (2010).
17. S. Yokoyama, S. Tajima, and A. Yamamoto, J. Biochem. **91,** 1267 (1982).
18. R. I. Litvinov, H. Shuman, J. S. Bennett, and J. W. Weisel, Proc. Natl. Acad. Sci. **99,** 7426 (2002).
19. E. Evans, K. Kinoshita, S. Simon, and A. Leung, Biophys. J. **98,** 1458 (2010).
20. E. A. Evans and D. A. Calderwood, Science **316,** 1148 (2007).
21. G. Bell, Science **200,** 618 (1978).
22. E. Evans, K. Halvorsen, K. Kinoshita, and W. P. Wong, Handbook of Single-Molecule Biophys. **20,** 571 (2009).
23. W. Hanley, O. McCarty, S. Jadhav, Y. Tseng, D. Wirtz, and K. Konstantopoulos, J. Biol. Chem. **278,** 10556 (2003).
24. P. M. Williams, Analytica Chimica Acta. **479,** 107 (2003).
25. M. L. Fitzgerald, K. Okuhira, G. F. Short III, J. J. Manning, S. A. Bell, and M. W. Freeman, J. Biol. Chem. **279,** 48477 (2004).
26. D. W. Scott, Biometrika **66,** 605 (1979).